ORIGINAL ARTICLE

JBMR

Volumetric DXA (VXA): A New Method to Extract 3D Information From Multiple In Vivo DXA Images

Omar Ahmad,[1] Krishna Ramamurthi,[2] Kevin E Wilson,[2] Klaus Engelke,[3] Richard L Prince,[4] and Russell H Taylor[1]

[1]Engineering Research Center for Computer-Integrated Surgical Systems and Technology, Departments of Computer Science, Mechanical Engineering, and Radiology, The Johns Hopkins University, Baltimore, MD, USA

[2]Hologic, Inc., Bedford, MA, USA

[3]Institute of Medical Physics, University of Erlangen, Erlangen, Germany

[4]School of Medicine and Pharmacology, University of Western Australia and Department of Endocrinology and Diabetes, Sir Charles Gairdner Hospital, Perth, Western Australia

ABSTRACT

Three-dimensional geometric and structural measurements of the proximal femur are of considerable interest in understanding the strength of the femur and its susceptibility to fracture. Quantitative computed tomography (QCT) with a small voxel size ($\leq$1 mm per side) is the current "gold standard" to examine the macrostructure of the femur, but it has a high effective radiation dose (approximately 2 to 5 mSv) and cost. Volumetric dual-energy X-ray absorptiometry (VXA) uses a commercially available DXA system (Hologic Discovery A) to reconstruct the proximal femur from four DXA scans delivering an effective radiation dose of 0.04 mSv. VXA was compared with QCT (voxel size of $0.29 \times 0.29 \times 1$ mm) in 41 elderly women (age 82 ± 2.4 years) at slices located at the femoral neck and trochanteric regions of interest. For parameters of shape, the femoral neck axis length (FNAL) and the cross-sectional slice area (SA), accuracy and strong linear correlations ($r = 0.84$ to 0.98) were demonstrated. Similar correlations ($r = 0.81$ to 0.97) were observed for the density parameters, the cross-sectional bone area (CSA) and volumetric bone mineral density (vBMD). VXA also demonstrated strong correlations ($r = 0.76$ to 0.99) for the engineering parameters of the minimum, maximum, and polar cross-sectional moments of inertia (CSMIs) and the section modulus (Z). We conclude that VXA is capable of generating a variety of 3D geometric and structural measurements that are highly correlated with QCT in elderly subjects in vivo. Moreover, the VXA measurements can be made with a commercially available DXA device at a very low radiation dose. © 2010 American Society for Bone and Mineral Research.

KEY WORDS: HIP STRUCTURE ANALYSIS; DXA; BONE DENSITOMETRY; QCT; BONE STRUCTURE

Introduction

Proximal femur areal bone mineral density (aBMD, g/cm^2) measured by dual-energy X-ray absorptiometry (DXA) has been shown in many prospective studies to be a major predictor of fracture risk.[1] As such, it is the current clinical standard for the diagnosis of osteoporosis. Furthermore, DXA is inexpensive, has a very low radiation dose (effective dose of less than 0.01 mSv), and has been shown to be cost-effective for the management of bone disease.[2,3] Nevertheless, as a measure of the structural integrity of bone, DXA has limitations. DXA is a 2D projection measurement of a 3D object, which limits the geometric and structural information that can be derived from a DXA exam and may, in turn, limit its ability to predict fracture risk. This may account, in addition to the propensity to fall, for the fact that that more than half of women who suffer a hip fracture do not have low aBMD as measured by DXA.[4–6]

Because quantitative computed tomography (QCT) provides a 3D measurement at moderately high resolution (voxels $\leq$ 1 mm in all dimensions), it is considered the "gold standard" for measurements of bone macrostructure. However, the radiation dose required for moderately high-resolution QCT (effective dose 2 to 5 mSv), along with the high cost of such measurements, has to date limited QCT's use primarily to research studies.[7]

There has long been a desire to obtain 3D geometric and structural information about bone from a few 2D X-ray images. If this goal were achievable, it would circumvent the high-dose, high-cost, and access limitations associated with QCT. Volumetric reconstruction of an arbitrary object sampled with d pixels requires about $\pi d/4$ images, for example, 200 images for a matrix

Received in original form March 23, 2010; revised form April 21, 2010; accepted May 24, 2010. Published online June 7, 2010.
Address correspondence to: Kevin E Wilson, Hologic, Inc., 35 Crosby Drive, Bedford, MA 01730, USA. E-mail: kwilson@hologic.com

Journal of Bone and Mineral Research, Vol. 25, No. 12, December 2010, pp 2468–2475
DOI: 10.1002/jbmr.140

of 256^2 pixels. However, if one has a priori knowledge of the object to be measured, multiple methods have been postulated for volumetric image reconstruction of the object with fewer 2D images. These methods have been an active area of research for many years.[8–14] DXA images are particularly well suited for limited field-of-view image-reconstruction methods of the skeleton because the soft tissue can be subtracted from the patient image, greatly reducing image complexity. This report is the first to examine in vivo the correlation with QCT of structural and geometric parameters obtained from volumetric DXA (VXA) constructed from four DXA images.

Materials and Methods

Study subjects

Forty-eight subjects for this study were recruited at random from the CAIFOS Age Related Extension (CARE) study, a population-based study of ambulatory elderly women. The only exclusions were focal bone disease or osteomalacia.[15,16] The mean age of participants was 82.8 (SD 2.5) years, height was 157.4 (6.1) cm, weight was 64.2 (10.7) kg, and body mass index (BMI) was 25.9 (3.9) kg/m^2. Informed consent was obtained from each patient, and the study was approved by the Sir Charles Gardiner Hospital Ethics Committee.

Data acquisition

The VXA measurements consisted of four DXA images of the proximal femur taken with a Discovery A bone densitometer (Hologic, Inc., Bedford, MA, USA) at –21, 0, 20, and 30 degrees, where the angle is measured relative to the posteroanterior image (0 degrees). The total effective radiation dose was 0.04 mSv.[17] QCT of the same hip was measured on the same day as the VXA using a 64-slice Phillips CT Brilliance 64 (Phillips Healthcare, Best, The Netherlands) with a Mindways calibration phantom (Mindways Software, Inc., Austin, TX, USA) placed below the patient. The QCT technique factors were 120 kV, 170 mA, pitch of 1, 1-mm slice thickness, reconstruction kernel B, and 15-cm reconstruction field of view, resulting in a 0.29-mm in-plane voxel size. Total effective radiation dose was 4 mSv. Periosteal and endosteal bone surfaces of the QCT images were segmented using the Medical Image Analysis Framework (MIAF) software package developed at the University of Erlangen.[18] Four subjects did not have the proximal femur scanned appropriately, 1 scan file was corrupted during data transfer, and in 2 cases the femurs were not segmented successfully, yielding 41 subjects with complete data for this analysis.

Development of the proximal femur atlas

In this study, the limited information from the four DXA images available for mathematical image reconstruction of the proximal femur was supplemented by incorporating information from a statistical model or atlas created using software developed at Johns Hopkins University.[8,14] The data for the atlas came from the QCT scans of 99 white women aged over 65 years acquired with a Siemens Sensation 64 (Siemens Medical Systems, Erlangen, Germany) and used the same acquisition as described earlier but used the B40s reconstruction kernel. The entry and exclusion criteria for these women, who were a subset of the Erlangen Senior Fitness and Prevention Study (SEFIP), have been published previously.[19]

A proximal femur statistical atlas was generated by fitting a tetrahedral model with shape and density information onto each subject's segmented proximal femur QCT scan.[20] From these individual models, an average tetrahedral femur model was derived. Deformation fields then were calculated from this average femur model to each subject's tetrahedral model. Principal-components analysis was performed on the deformation fields to calculate the principal modes of variation. This allowed the most important features of the shape and density of the atlas to be summarized by using the average femur along with a discreet number of modes of variation. In this analysis, we used eight modes of variation.

VXA method

The VXA method reported here extends earlier work on "deformable" 2D/3D registration of statistical atlases of bony anatomy to X-ray images.[13,21–24] The method is an iterative process (Fig. 1). The four DXA images are compared with projections of an iteratively modified tetrahedral subject model. The process begins by assuming an average femur derived from the femur atlas. At each iteration, the pose (location and orientation in space), scale, and modes of variation of the statistical model are varied to minimize the difference between the simulated DXA images from projections of the model and the actual acquired DXA images. Thousands of iterations are performed, and the summed mutual information of the four images is minimized. The resulting tetrahedral model of the subject's femur, when projected into the four angles measured by DXA, closely approximates the DXA images, particularly for shape and, to a lesser extent, for density. To better approximate the subject's femur density, as a final step, aBMD in each pixel of the posteroanterior VXA projection calculated from the subject's model is calibrated to the measured aBMD value in the posteroanterior DXA image. The BMD values of all voxels in the model contributing to the projected pixel were linearly scaled so that the aBMD of the projected pixel was equal to the measured aBMD of corresponding pixel in the posteroanterior DXA image. The voxel density was calibrated to DXA based on the value for cortical bone from the National Institute of Standard and Technology (NIST) (1850 mg/cm^3).

The completed VXA image is a volumetric model of the subject's proximal femur containing patient specific shape and volume information (Fig. 2) identical in format to a segmented QCT image. By construction, the subject's VXA image is located in DXA space with a known pose with respect to the densitometer. However, the QCT image is located in CT space, and the orientation of the patient femur is likely different than for the DXA measurement. For accurate comparison, the segmented QCT image of each subject's proximal femur was fitted with a tetrahedral mesh, and the QCT image then was transformed to DXA space by changing the pose of the QCT image until four simulated DXA images from projections of the QCT image minimized the difference with the four DXA images taken in the

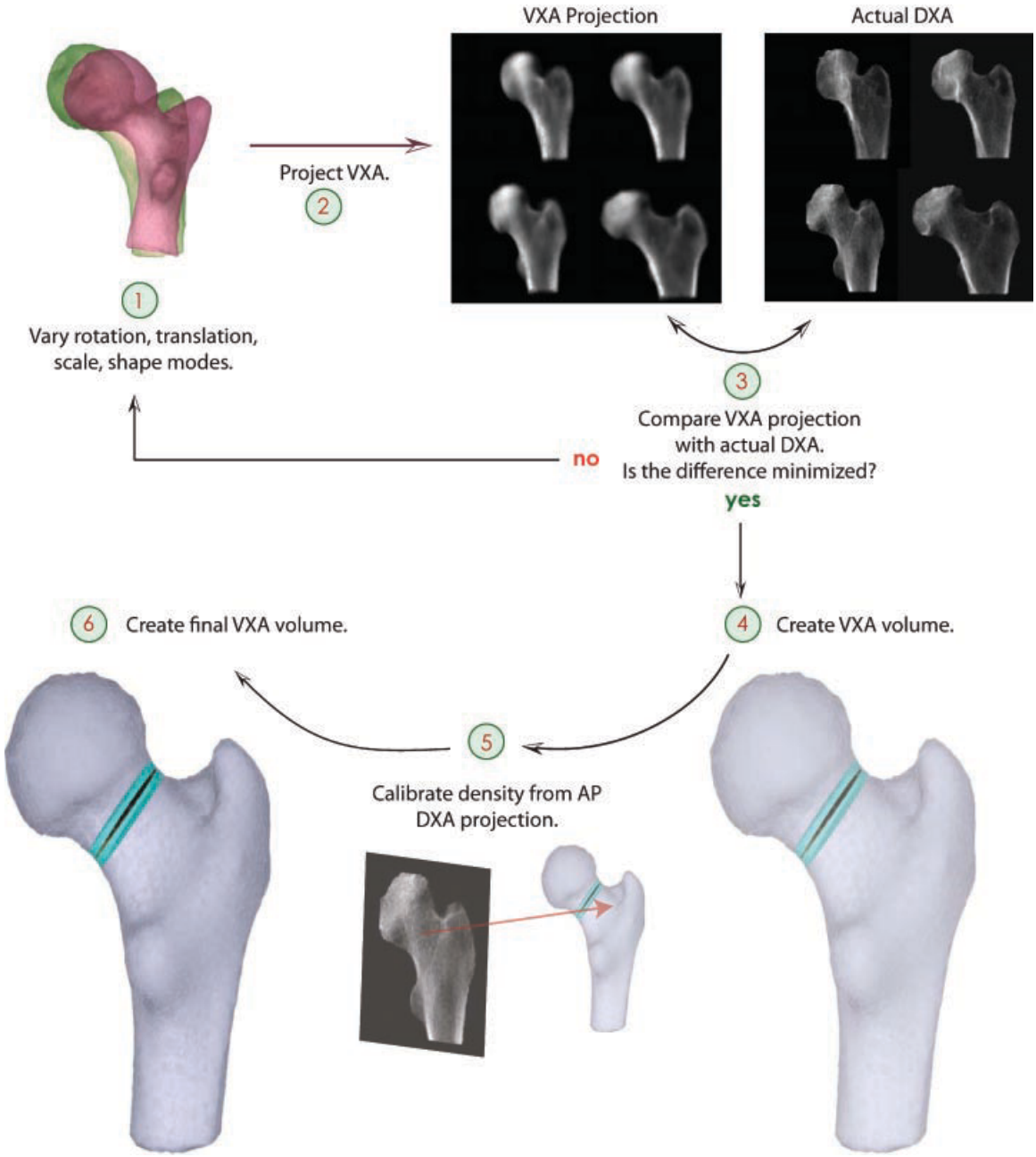

Fig. 1. Diagrammatic description of the development of the VXA model.

VXA acquisition. This allows comparison between VXA and QCT without the confounder of different regions of interest (ROIs). An ROI chosen on the posteroanterior DXA image can be placed accurately on the VXA and QCT volumes because they are aligned with this image.

Regions of interest (ROIs) and measured parameters

Primarily two ROIs are used in this article. Both are 1-mm-thick slices that are perpendicular to the plane defined by the posteroanterior DXA image and correspond to the narrow neck (NN) and the intertrochanteric (IT) regions used for Hip Structure Analysis (HSA) analysis in DXA (APEX Version 3.0, Hologic, Bedford, MA, USA). On the DXA image the NN ROI cuts through the center of the femoral neck, whereas the IT ROI is through the greater trochanter (Fig. 2). Additionally, a third ROI, the minimal neck area, was defined as the plane through the femoral neck that had minimal area. Unlike the other two ROIs, this minimal neck area ROI was found independently on the VXA and QCT images and was not in general perpendicular to the posteroanterior DXA image.

All reported parameters [ie, femoral neck axis length (FNAL); slice area (SA); cross-sectional area of bone (CSA); volumetric BMD (vBMD); the polar, minimum, and maximum cross-sectional moment of inertia (CSMI); and the section modulus (*Z*)], used the same algorithm for the QCT and VXA images and are defined in detail in the Appendix. QCT was considered the "gold standard," and VXA was compared with QCT by linear regression analysis.

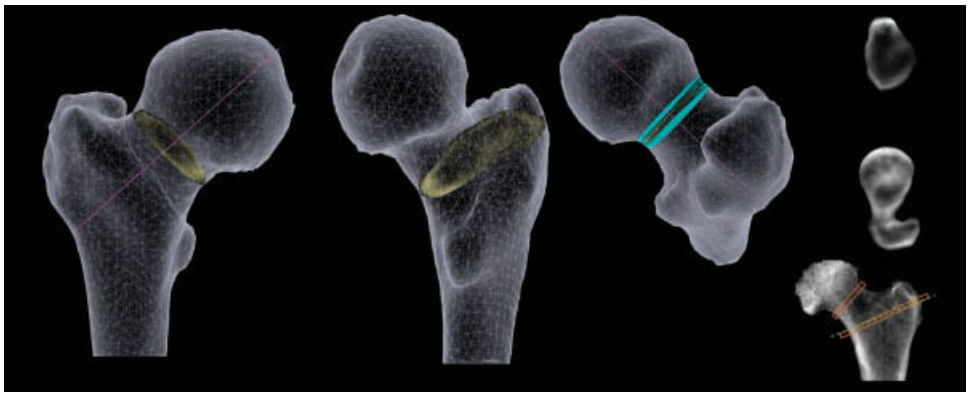

Fig. 2. Volume rendering of a VXA image showing the sections and lengths measured and two cross-sectional slices showing density distribution. On the image on the left, the femoral neck axis length (*purple line*) and the narrow neck (NN) region (*yellow shading*; darker yellow indicates higher density) are shown. The middle image shows the slice through the intertrochanteric (IT) region. The blue volume on the third image from the left shows the size of a slab used for the narrow neck vBMD calculation. The two images on the upper far right are cross-sectional slices with density indicated by brightness and on the bottom right is the posteroanterior DXA image with the NN and IT regions shown.

Results

VXA QCT structural comparisons

For the structural variables of FNAL, SA, CSA, and vBMD, high linear correlations were demonstrated for all of the ROIs ($r = 0.81$ to 0.98), as shown in Fig. 3. The slopes and offsets of the linear regressions for the regions are reported in Table 1. The length of the FNA was the same for VXA and QCT. The SA was slightly larger (2% to 9%) with VXA. For the NN and IT regions, the offset of the regression for SA did not reach statistical significance ($p = .34$ and $p = .12$, respectively), but for the combined regions, the offset was highly significant ($p < .01$).

The regressions of the parameters that contained density, CSA, and vBMD indicated that a slope and offset are required to cross-calibrate between VXA and QCT. This is not surprising because VXA was calibrated to DXA aBMD calibration standards, which were different from the QCT calibration standard.

VXA QCT engineering comparisons

As shown in Fig. 4, strong correlation also was observed for all regions for engineering parameters that measure resistance to bending forces, CSMI, $CSMI_{min}$, $CSMI_{max}$, and Z (r varied from 0.76 to 0.99). $CSMI_{min}$ showed lower correlations than the other parameters and was the only engineering parameter with a statistically significant offset ($0.18 \pm 0.05\ cm^4$) for the combined data.

The correlation of VXA and QCT also was examined at the minimal neck area ROI. However, this ROI did not give statistically different results from the NN ROI for the r value for any of the reported parameters (data not shown).

Discussion

This study is unique in its methodology and is the first to report on truly 3D density-based parameters acquired in vivo by a DXA scanner. Strong correlations with minimal offset were observed between shape and structural parameters calculated by VXA and QCT in the femoral neck and trochanteric regions of the femur. This finding demonstrates that both the shape and density of the VXA model strongly correlate with the QCT of the subject's femur in these regions. The femoral neck and trochanteric regions are of particular interest because they are the regions where most femoral fractures occur, and femoral fractures are the most severe consequence of osteoporosis.

A strength of the method used in this study is that the model was fit using both the shape and density of the complete proximal femur. Thus, even areas of the femur outside the region of interest assist in constraining the measured regions. When the shape of VXA was compared with QCT, a small systematic overestimation of the physical cross-sectional area of the femoral neck of 9% and, to a lesser extent (2%), the trochanteric region was observed. This overestimation was not seen in the FNAL parameter, which measures a distance approximately in the plane of the posteroanterior image. This is likely due to the limited angles available to DXA because there is no angle that provides a good constraint on the posteroanterior depth of the femoral neck. It would be highly desirable to obtain greater angular coverage so as to have at least a 90-degree angular range between the two most separated DXA images. However, this study used the maximum angle obtainable on the only C-arm densitometer available commercially, which is 51 degrees. Additionally, this angular separation also approaches the practical limit imposed by patient anatomy because angular separation beyond about 60 degrees will be obscured either by the contralateral femur or the acetabulum.

At its current stage of development, VXA does not allow separation between the cortical and trabecular components of the bone, nor is the width of the cortex modeled accurately (Fig. 2). This limitation is shared by low-resolution QCT, where the voxel size is larger than the cortical width. Even with the higher-resolution QCT approach used in this study, certain cortical widths, such as at the upper femoral neck, are not measured reliably. A future area of research, which potentially could allow VXA to accurately model the cortical and trabecular components separately, would be to explicitly include the cortical and trabecular segmentation during the construction of the VXA atlas

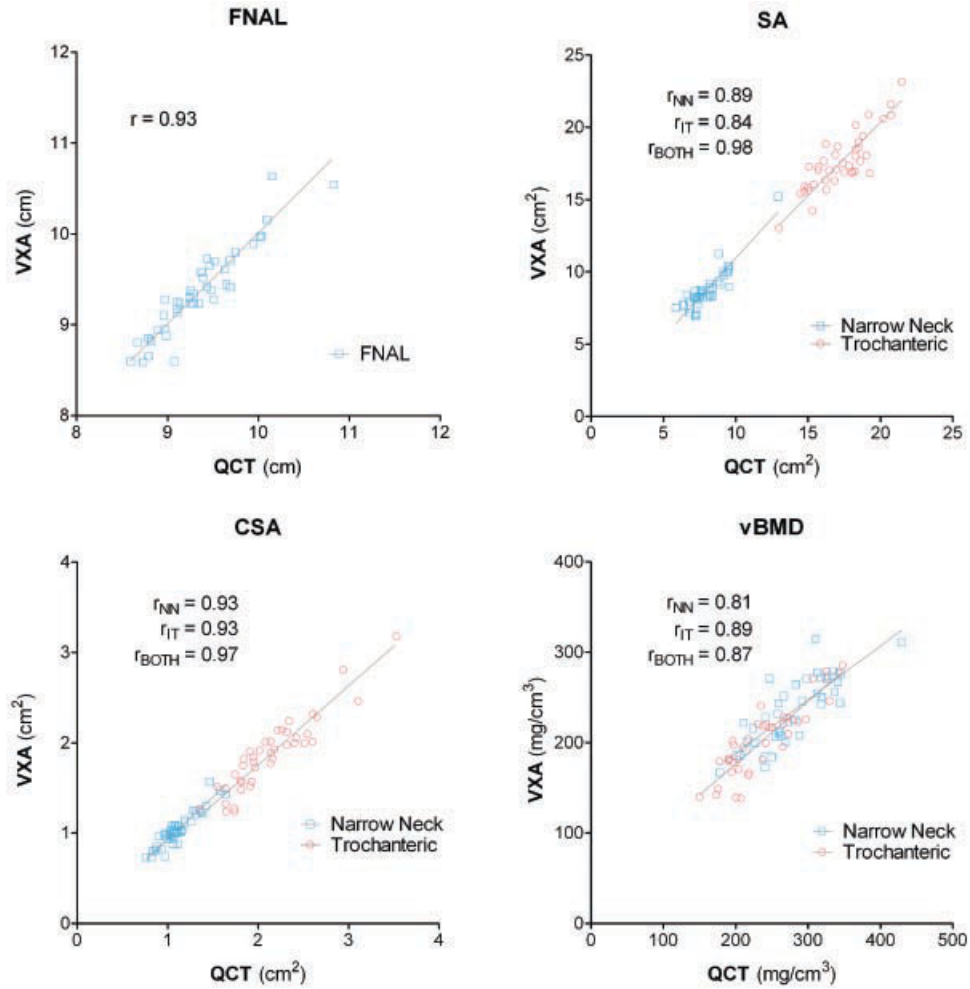

Fig. 3. VXA versus QCT for the structural parameters. FNAL was found independently on VXA and QCT, whereas SA, CSA, and vBMD used the NN and IT regions defined from the posteroanterior DXA image with APEX 3.0 HSA software.

along with the use of smaller tetrahedrons or a different model representation. One then could investigate whether the relatively low-resolution DXA images currently used clinically provided sufficient constraint to separate cortical and trabecular bone accurately.

An additional consideration is that VXA is model-dependent. The accuracy of the reconstructed VXA volume depends on whether the VXA atlas has modes of variation that contain the anatomic uniqueness of the patient. In this study, good success was found in predicting elderly white Australian women from less elderly white German women. Further work will be required to determine whether men or other ethnicities can be modeled with this atlas or whether gender- and ethnicity-specific atlases will need to be created.

This study has a number of strengths. First, it was an in vivo study of elderly women in whom bone mass was low. Therefore, it is expected that translation of the method to somewhat younger individuals who typically have higher bone mass, fewer degeneracies, and better-defined structure is likely to be less difficult. Second, results were compared with QCT taken at a relatively high spatial resolution. In particular, the slice thickness of 1 mm was much thinner than the 3 mm used in many QCT protocols. Third, the software used to calculate the parameters of the VXA and QCT volumes was identical, thus eliminating any possible algorithmic differences. Fourth, the VXA and QCT volumes were coregistered, so region placement differences were eliminated. Finally, a number of geometric and density parameters were compared in the two most important fracture regions of the proximal femur, and strong correlations were observed for all these parameters.

It also must be emphasized that the sample size was relatively small and designed to study technical aspects of a new technology rather than VXA's ability to predict fracture.

There are several potential advantages of VXA over QCT. The cost of installation and servicing of a DXA device is far less than for QCT. In addition, most patients evaluated for osteoporosis are already referred for DXA BMD measurements, so the additional burden of obtaining 3D data on the same device is minimal in terms of subject scheduling and the total time required per study subject. Finally, achieving accurate 3D shape and structural measurements using four DXA images on a commercially available bone densitometer required an effective dose that was 100 times smaller than the dose delivered by QCT. Even with more advanced dose-reduction techniques now available for

Table 1. Results of Linear Correlation of VXA versus QCT at the Narrow Neck Region, the Intertrochanter Region, and Combined Regions

	Narrow neck	Intertrochanter	Combined
Femoral Neck Axis Length (cm)			
r	0.93	—	—
Offset	N.S.	—	—
Slope	1.001 (0.003)	—	—
Slice area (cm^2)			
r	0.89	0.84	0.98
Offset	N.S.	N.S.	1.2 (0.3)
Slope	1.09 (0.01)	1.02 (0.01)	0.95
Cross-sectional area (cm^2)			
r	0.93	0.93	0.97
Offset	N.S.	N.S.	0.11 (0.04)
Slope	0.93 (0.01)	0.88 (0.01)	0.83 (0.02)
vBMD (mg/cm^3)			
r	0.81	0.89	0.87
Offset	69 (19)	38 (14)	48 (11)
Slope	0.59 (0.07)	0.69 (0.06)	0.66 (0.04)

Note: Numbers in parenthesizes are standard error. N.S. indicates that the offset (ie, intercept) was not significantly different from zero, in which case the slope is reported with the offset fixed to zero. The linear coefficient *r* is reported with the offset not fixed to zero.

QCT, a difference of a factor of 30 to 50 would remain. Radiation dose is an increasing concern both to the public and to institutional review boards.

The closest study to the present one is by Kolta and colleagues[10] using cadaver femurs and comparing multiple DXA and QCT images. Kolta and colleagues studied 25 human cadavers using a Delphi W (Hologic) and a special fixture that allowed the femur to be rotated by 90 degrees for the two acquired images. To translate their method to a practical in vivo method that could be performed on a commercial densitometer would require overcoming multiple problems. Perhaps the most serious problem to overcome would be that one of their two DXA images was a lateral image of the femur, which in vivo would be obscured by the contralateral femur and pelvis. Another significant difference between our method and the method used by Kolta and colleagues is that their method only models the shape of the femur, not its density. This excludes the possibility of calculating many important structural parameters such as CSMI, *Z*, and vBMD. Finally, Kolta and colleagues did not report comparisons of FNAL and SA with QCT, so a direct comparison with our in vivo study is not possible.

We conclude that VXA may be a promising technology for in vivo measurements of a variety of 3D shape and macrostructural measurements of the proximal femur in elderly white women. The technique is also more convenient and cost-effective than QCT and uses a significantly lower effective dose. The fact that it can be undertaken using equipment currently available to clinicians also makes it an attractive proposition. However, further studies will be required to establish it as a viable alternative to QCT in research and clinical practice. In relation to the true clinical advantage of VXA over CT and DXA, the "gold standard" will require demonstration of increased predictive power of fracture events. In the meanwhile, case-control comparisons of predictive power using receiver operating characteristic (ROC) analysis in fracture and nonfracture patients will be of great interest.

Disclosures

OA received research support from Hologic, Inc. KR is an employee of Hologic, Inc. KEW is an employee of Hologic, Inc. KE received research support from Hologic, Inc. RHT received research support from Hologic, Inc. OA, KR, KEW, and RHT had full access to the all the data for this study, and RLP and KE had full access to the raw data tables and analysis.

Acknowledgments

This study was funded by Hologic, Inc.

Appendix

The parameters reported in this study were defined as follows:

Slice area (SA, cm^2) is the area defined by the outer dimension of the periosteal boundary of the cross section of the slice.

Cross-sectional area (CSA, cm^2) is the area of the slice defined as bone. Thus the area of each pixel is weighted by the amount of bone in the pixel.

Cross-sectional moment of inertia (CSMI, cm^4) for a slice is a two-component vector. If $\rho(x, y)$ is the volumetric bone density in mg/cm^3 per voxel in the slice and $\rho_{NIST} = 1850\,mg/cm^3$, (x_{CM}, y_{CM}) is the location of the center of mass. Define the center of mass coordinate system as

$$\hat{x} = (x - x_{CM})$$
$$\hat{y} = (y - y_{CM})$$

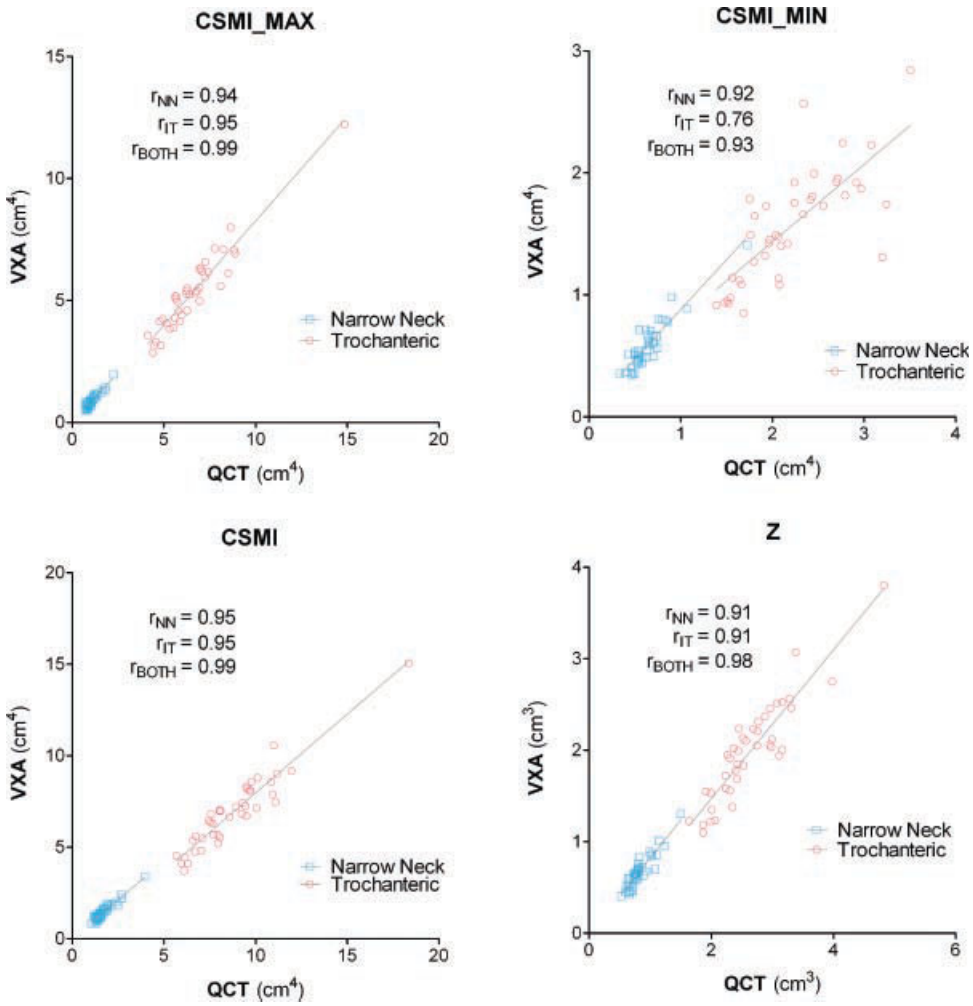

Fig. 4. VXA versus QCT for the engineering parameters of the slices in the narrow neck and trochanteric regions.

Then

$$\mathrm{CSMI}_x = \iint \hat{y}^2 \left(\frac{\rho(x,y)}{\rho_{\mathrm{NIST}}}\right) dxdy$$

$$\mathrm{CSMI}_y = \iint \hat{x}^2 \left(\frac{\rho(x,y)}{\rho_{\mathrm{NIST}}}\right) dxdy$$

$$\mathrm{CSMI}_{xy} = \iint \hat{x}\hat{y} \left(\frac{\rho(x,y)}{\rho_{\mathrm{NIST}}}\right) dxdy$$

and

$$\mathrm{CSMI} = \mathrm{CSMI}_x + \mathrm{CSMI}_y$$

$$\mathrm{CSMI}_{\max} = \frac{\mathrm{CSMI}}{2} + \sqrt{\left[(\mathrm{CSMI}_x - \mathrm{CSMI}_y)/2\right]^2 + \mathrm{CSMI}_{xy}^2}$$

$$\mathrm{CSMI}_{\min} = \frac{\mathrm{CSMI}}{2} - \sqrt{\left[(\mathrm{CSMI}_x - \mathrm{CSMI}_y)/2\right]^2 + \mathrm{CSMI}_{xy}^2}$$

Thus CSMI without a subscript is the polar CSMI with the origin located at the center of mass. $\mathrm{CSMI}_{\max}$ and $\mathrm{CSMI}_{\min}$ are the minimum and maximum values of CSMI. The $\rho(x, y)/\rho_{\mathrm{NIST}}$ term defines the bone fraction within a pixel and accounts for partial-volume effects of the finite voxel size. This definition of the moment of inertia is consistent with that defined by Martin and colleagues[25] and is consistent with what is reported by HSA in the published literature.

Section modulus (*Z*, cm^3) is $\mathrm{CSMI}/r_{\max}$.

vBMD ($\mathrm{mg/cm}^3$) is the volumetric density of the ROI for a 10-mm-thick slab centered on the ROI slice.

Femoral neck axis length (FNAL, cm) is perpendicular to the narrowest plane of the femoral neck. The length of the axis was through the center of mass to the edge of the femoral head where the axis exited the femur proximally. To reduce noise introduced by osteophytes, the FNAL was the median value of the nine line segments, all parallel to the neck axis but equally distributed around the neck axis in a circle with a 1-mm radius.

References

1. Marshall D, Johnell O, Wedel H. Meta-analysis of how well measures of bone mineral density predict occurrence of osteoporotic fractures. BMJ. 1996;312:1254–1259.
2. Schott AM, Ganne C, Hans D, et al. Which screening strategy using BMD measurements would be most cost effective for hip fracture prevention in elderly women? A decision analysis based on a Markov model. Osteoporos Int. 2007;18:143–151.
3. Schousboe JT, Ensrud KE, Nyman JA, Melton LJ 3rd, Kane RL. Universal bone densitometry screening combined with alendronate therapy

for those diagnosed with osteoporosis is highly cost-effective for elderly women. J Am Geriatr Soc. 2005;53:1697–1704.

4. Schuit SC, van der Klift M, Weel AE, de Laet CE, Burger H, Seeman E. Corrigendum: "Fracture incidence and association with bone mineral density in elderly men and women: the Rotterdam Study." Bone. 2006;38:603.
5. Schuit SC, van der Klift M, Weel AE, et al. Fracture incidence and association with bone mineral density in elderly men and women: the Rotterdam Study. Bone. 2004;34:195–202.
6. Wainwright SA, Marshall LM, Ensrud KE, et al. Hip fracture in women without osteoporosis. J Clin Endocrinol Metab. 2005;90:2787–2793.
7. Black DM, Bouxsein ML, Marshall LM, et al. Proximal femoral structure and the prediction of hip fracture in men: a large prospective study using QCT. J Bone Miner Res. 2008;23:1326–1333.
8. Chintalapani G, Ellingsen LM, Sadowsky O, Prince JL, Taylor RH. Statistical atlases of bone anatomy: construction, iterative improvement and validation. Med Image Comput Comput Assist Interv 10(Pt 1). 2007; 499–506.
9. Gueziec A, Kazanzides P, Williamson B, Taylor RH. Anatomy-based registration of CT-scan and intraoperative X-ray images for guiding a surgical robot. IEEE Trans Med Imaging. 1998;17:715–728.
10. Kolta S, Le Bras A, Mitton D, et al. Three-dimensional X-ray absorptiometry (3D-XA): a method for reconstruction of human bones using a dual X-ray absorptiometry device. Osteoporos Int. 2005;16:969–976.
11. Laporte S, Skalli W, de Guise JA, Lavaste F, Mitton D. A biplanar reconstruction method based on 2D and 3D contours: application to the distal femur. Comput Methods Biomech Biomed Engin. 2003;6:1–6.
12. Le Bras A, Kolta S, Soubrane P, Skalli W, Roux C, Mitton D. Assessment of femoral neck strength by 3-dimensional X-ray absorptiometry. J Clin Densitom. 2006;9:425–430.
13. Yao J. A statistical bone density atlas and deformable medical image registration Computer Science, vol. PhD. Johns Hopkins University, Baltimore. 2002.
14. Yao J, Taylor RH. Non-Rigid Registration and Correspondence in Medical Image Analysis Using Multiple-Layer Flexible Mesh Template Matching. IJPRAI. 2003;17:1145–1165.
15. Prince RL, Devine A, Dhaliwal SS, Dick IM. Effects of calcium supplementation on clinical fracture and bone structure: results of a 5-year, double-blind, placebo-controlled trial in elderly women. Arch Intern Med. 2006;166:869–875.
16. Zhu K, Devine A, Prince RL. The effects of high potassium consumption on bone mineral density in a prospective cohort study of elderly postmenopausal women. Osteoporos Int. 2009;20:335–340.
17. Blake GM, Naeem M, Boutros M. Comparison of effective dose to children and adults from dual X-ray absorptiometry examinations. Bone. 2006;38:935–942.
18. Kang Y, Engelke K, Fuchs C, Kalender WA. An anatomic coordinate system of the femoral neck for highly reproducible BMD measurements using 3D QCT. Comput Med Imaging Graph. 2005;29:533–541.
19. Kemmler W, von Stengel S, Engelke K, Haberle L, Kalender WA. Exercise effects on bone mineral density, falls, coronary risk factors, and health care costs in older women: the randomized controlled senior fitness and prevention (SEFIP) study. Arch Intern Med. 170:179–185.
20. Ahmad O, Ramamurthi K, Wilson KE, Engelke K, Bouxsein ML, Taylor RH. 2009. 3D Structural Measurements of the Proximal Femur from 2D DXA Images Using a Statistical Atlas SPIE Medical Imaging, vol. 7260, Orlando, FL.
21. Sadowsky O. Image Registration and Hybrid Volume Reconstruction of Bone Anatomy Using a Statistical Shape Atlas Computer Science, vol. PhD. Johns Hopkins Univerity, Baltimore. 2008.
22. Sadowsky O, Chintalapani G, Taylor RH. Deformable 2D-3D registration of the pelvis with a limited field of view, using shape statistics. Med Image Comput Comput Assist Interv. 2007;10 (Pt 2): 519–526.
23. Sadowsky O, Cohen JD, Taylor RH. Projected tetrahedra revisited: a barycentric formulation applied to digital radiograph reconstruction using higher-order attenuation functions. IEEE Trans Vis Comput Graph. 2006;12:461–473.
24. Yao J, Taylor RH. 2002. Deformable registration between a statistical bone density atlas and X-ray images Second International Conference on Computer Assisted Orthopaedic Surgery (CAOS 2002), Santa Fe, NM.
25. Martin RB, Burr DB. Non-invasive measurement of long bone cross-sectional moment of inertia by photon absorptiometry. J Biomech. 1984;17:195–201.